The quantification and forecasting of magnetic complexity in solar active regions

Stephen J. Bannister and D. Shaun Bloomfield

Department of Mathematics, Physics and Electrical Engineering, Northumbria University, Newcastle upon Tyne, UK

Northumbria University NEWCASTLE

1. Introduction/motivation

Active regions (ARs) are distinct regions of the Sun where sub-surface kG magnetic flux has emerged. They store vast amounts of energy and are sites of magnetic reconnection, the main driver for solar flares. A common way of classifying ARs with sunspots is the **Mt. Wilson magnetic classification scheme**[1;2]. Classes are separated by magnetic morphology, declared every 24 hours at 00:30 UT by SWPC. A downside to this system is that *two ARs with the same class can be vastly different in their magnetic complexities*. We show the advantages of **quantifying this complexity**, using the `hmi.sharp_cea_720s` data series[3] from the HMI[4] instrument on-board NASA's SDO[5] satellite.

2. Sunspot/pore feature detection

We are interested in classifying a feature as anything with a magnetic field strength significant enough to inhibit subsurface convection and cause darkening in the photosphere such as **umbrae & pores**. To consistently detect features, an algorithm was established c.f. Padinhatteeri et al. (2016)[6]. Before applying the feature extraction algorithm, we first correct the continuum for limb darkening effects and normalize to the quiet Sun (I_{QS}, median). The parameters & arguments of the algorithm are:

Longitude: ±75° **Intensity**: 0.67 I_{QS} **Min. Area**: 7 px **Separation**: 4 px

3. Polarity Inversion Measure (PIM)

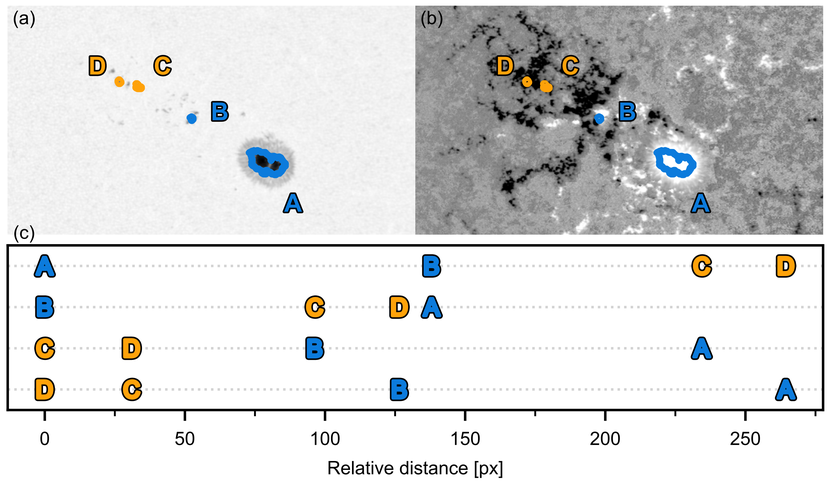

To quantify magnetic complexity of ARs, we introduce our Polarity Inversion Measure (PIM). Using the features extracted algorithmically in §2, the steps to calculate PIM are:

- Calculate geometric centroid of all N features (panel a)
- Extract mag. polarity (n or p) & flux of features using the cotemporal B_R magnetogram (panel b)
- Using geometric centroids of each feature, calculate the distance to every other feature
- Order list of features by distance from starting feature (panel c)
- PI_i is the number of polarity inversions (PIs) in this list i.e. how many $p \longleftrightarrow n$ transitions exist
- Repeat using each feature i as a unique starting point
- PIM is the average over all N starting features (unweighted PIM) or N_ϕ flux (flux-weighted PIM)

PIM for the AR in the example Figure (left) is demonstrated here. Starting from **A**, the polarity inverts once (from **B** → **C**) so $\mathrm{PI}_A = 1$. Similarly starting from **C** and **D** the polarity also inverts once (from **D** → **B** / **C** → **B**), so $\mathrm{PI}_{C,D} = 1$. Starting from **B**, there are two PIs (from **B** → **C** and **D** → **A**) so $\mathrm{PI}_B = 2$. Giving us a final (unweighted) PIM of,

$$\langle \mathrm{PIM} \rangle = \frac{1}{N}\sum_{i=0}^{N} \mathrm{PI}_i = \frac{5}{4} = 1.25$$

4. Statistical comparison to Mt. Wilson

We have performed a statistical analysis on 1530 HARP ARs containing only a single NOAA number between 2012–2024 inclusive. The IQR of PIM between 18:00–23:59 UT for each class is shown below, as we consider these the times that dominate SWPC's decision-making for the next day's class.

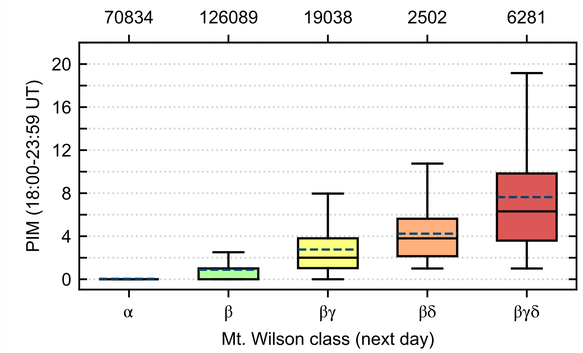

5. Mt. Wilson classification prediction

Expanding on §4, it appears that there is a statistical trend with PIM and the Mt. Wilson scheme where clearly **more complex classes have statistically higher PIM distributions**. Following on from this, we examine PIM's utility in forecasting Mt. Wilson class. In order to do this, we first examine each **starting class independently**. The below figures demonstrate the process from start to finish, showing the separate distributions' IQRs in the first figure and the corresponding Poisson statistics for likelihood to change class or stay the same in the second figure. From here, we built a training and testing set using all of the data from §4 (constrained and averaged between 19:00-21:00 UT) and trained models for each starting class by fitting sensible functions, similar to third figure. The resulting multi-category forecast contingency table is shown in the fourth figure, with forecast verification metrics given below.

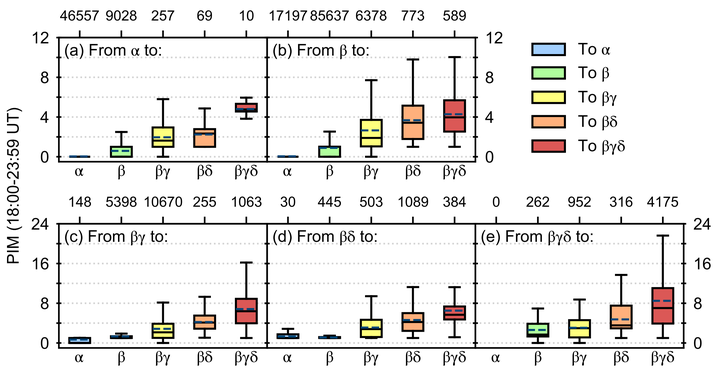

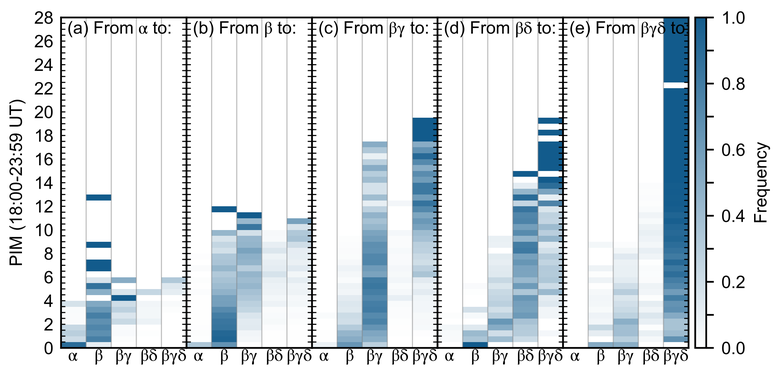

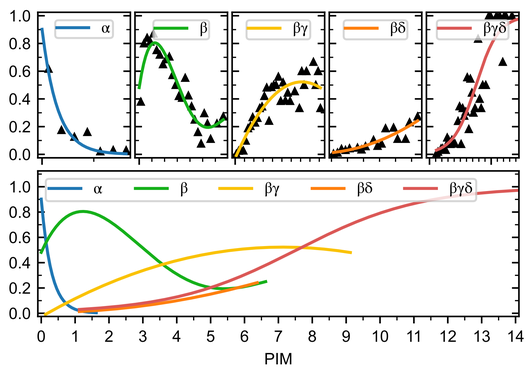

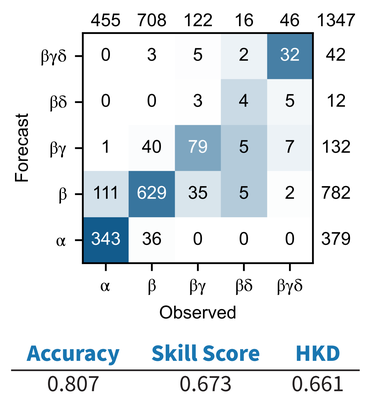

Accuracy	Skill Score	HKD
0.807	0.673	0.661

References

[1] Hale et al. (1919) *ApJ* **49** 153
[2] Künzel (1965) *AN* **288** 177
[3] Bobra et al. (2014) *Sol. Phys.* **289** 3549
[4] Schou et al. (2012) *Sol. Phys.* **275** 229
[5] Pesnell et al. (2012) *Sol. Phys.* **275** 3
[6] Padinhatteeri et al. (2016) *Sol. Phys.* **291** 41

Networking